Published as: *J Neurophysiol*. 2010 December ; 104(6): 3721–3731.

Validation of Independent Component Analysis for Rapid Spike Sorting of Optical Recording Data

Evan S. Hill[1,*], **Caroline Moore-Kochlacs**[2,*], **Sunil K. Vasireddi**[1], **Terrence J. Sejnowski**[2,3], and **William N. Frost**[1]

[1]Department of Cell Biology and Anatomy, The Chicago Medical School, Rosalind Franklin University of Medicine and Science, North Chicago, Illinois

[2]Howard Hughes Medical Institute, The Salk Institute for Biological Studies, University of California San Diego, La Jolla, California

[3]Division of Biological Sciences, University of California San Diego, La Jolla, California

Abstract

Independent component analysis (ICA) is a technique that can be used to extract the source signals from sets of signal mixtures where the sources themselves are unknown. The analysis of optical recordings of invertebrate neuronal networks with fast voltage-sensitive dyes could benefit greatly from ICA. These experiments can generate hundreds of voltage traces containing both redundant and mixed recordings of action potentials originating from unknown numbers of neurons. ICA can be used as a method for converting such complex data sets into single-neuron traces, but its accuracy for doing so has never been empirically evaluated. Here, we tested the accuracy of ICA for such blind source separation by simultaneously performing sharp electrode intracellular recording and fast voltage-sensitive dye imaging of neurons located in the central ganglia of *Tritonia diomedea* and *Aplysia californica*, using a 464-element photodiode array. After running ICA on the optical data sets, we found that in 34 of 34 cases the intracellularly recorded action potentials corresponded 100% to the spiking activity of one of the independent components returned by ICA. We also show that ICA can accurately sort action potentials into single neuron traces from a series of optical data files obtained at different times from the same preparation, allowing one to monitor the network participation of large numbers of individually identifiable neurons over several recording episodes. Our validation of the accuracy of ICA for extracting the neural activity of many individual neurons from noisy, mixed, and redundant optical recording data sets should enable the use of this powerful large-scale imaging approach for studies of invertebrate and suitable vertebrate neuronal networks.

INTRODUCTION

Large-scale optical recording with photodiode arrays and fast voltage-sensitive dyes (fVSDs) (Cohen and Salzberg 1978) can be used to simultaneously monitor the action potentials generated by dozens to hundreds of individual neurons. However, despite the

Address for reprint requests and other correspondence: E. S. Hill, Department of Cell Biology and Anatomy, The Chicago Medical School, Rosalind Franklin University of Medicine and Science, 3333 Green Bay Road, North Chicago, IL 60064 (evan.hill@rosalindfranklin.edu).
*These authors contributed equally to this work.

DISCLOSURES
No conflicts of interest, financial or otherwise, are declared by the author(s).

publication of several studies using this technique in both vertebrate (Neunlist et al. 1999; Obaid et al. 1999, 2005; Schemann et al. 2002; Vanden Berghe et al. 2001) and invertebrate preparations (Brown et al. 2001; Kojima et al. 2001; London et al. 1986, 1987; Nakashima et al. 1992; Nikitin and Balaban 2000; Wu et al. 1994a,b), it has been slow to gain widespread use.

A key reason for this has been the lack of an efficient, accuracy-verified spike sorting method for processing the complex optical data sets. A photodiode array used with an fVSD can collect hundreds of traces of action potential data. However, the larger neurons are typically redundantly recorded by several diodes and many diodes record the action potentials generated by multiple neurons. Such mixing and redundancy are unavoidable outcomes of recording methods using grid-based, extracellular detector arrays. The raw optical recordings can reveal the presence and location of neurons that fire during given motor programs—a major help for circuit mapping. However, to achieve the true promise of large-scale optical recording in invertebrates (Salzberg et al. 1977), an effective and validated spike sorting method is needed to analyze the simultaneous recording of >100 neurons that is possible with fVSDs.

One spike sorting method, spike template matching, was previously used by Cohen and colleagues to sort raw photodiode data obtained with fVSDs from invertebrate ganglia into single neuron traces (Falk et al. 1993; Hickie et al. 1997; Tsau et al. 1994; Wu et al. 1994a,b; Zecevic et al. 1989; Zochowski et al. 2000). This procedure required extensive operator involvement, leading to processing times of several days per record (Cohen et al. 1989). Further, the accuracy of this spike sorting method was not tested using simultaneously acquired intracellular recordings. [See Lewicki (1998) for a review of spike sorting techniques.]

More recently, independent component analysis (ICA), a blind source separation method well suited for analyzing neural time series data (Jung et al. 2001; Mukamel et al. 2009; Reidl et al. 2007; Siegel et al. 2007; Takahashi et al. 2003), was used to extract the spiking activity of many individual neurons from photodiode array data sets obtained from fVSD optical recordings of the central ganglia of the marine mollusk *Tritonia diomedea* (Brown et al. 2001, 2008). However, the accuracy of this ICA spike sorting was not evaluated using simultaneously acquired intracellular recordings.

ICA is a fully automated blind source separation procedure that transforms signal mixtures into a new set of candidate source signals called *components* that are statistically independent of one another. ICA makes no assumptions about how the source signals were mixed spatially and requires only that the underlying signals are non-Gaussian. The ICA algorithm we use, Infomax ICA (Bell and Sejnowski 1995; Brown et al. 2001), iteratively converges on a linear transformation of the data, which minimizes mutual information to maximize statistical independence between the resulting components. Mutual information is a statistical measure of the mutual dependence between signals. It quantifies how much information knowing the value of one signal provides about the value of another signal at any time. When applied to our 464-channel optical imaging data sets, Infomax ICA generates the same number of independent components, a subset of which contain the spiking activity of individual neurons, with the rest containing artifacts or noise.

The primary goal of the present study was to assess, for the first time, the accuracy of Infomax ICA for extracting individual neurons' action potentials obtained with optical recording and an fVSD. To accomplish this we used sharp electrodes to obtain intracellular recordings from neurons in the central ganglia of two invertebrate species, *Tritonia diomedea* and *Aplysia californica*, widely used for network studies (Cleary et al. 1995;

Cropper et al. 2004; Getting 1983; Popescu and Frost 2002), while simultaneously imaging neural activity with a 464-element photodiode array. We found that in 34 of 34 cases, the action potentials recorded from individual neurons with sharp electrodes corresponded exactly, spike-for-spike, to the optical spikes of one of the independent components returned by ICA. With currently available fast PC hardware, the time taken for ICA processing of 60- to 90-s optical data files from 464 channels sampled at 1,600 Hz is only a few minutes, making it possible to analyze optical data files during ongoing experiments. The combination of fVSD imaging and ICA allows us to routinely monitor the activity of dozens to >100 neurons in various ganglia of *Tritonia* and *Aplysia*. Our validation of the accuracy of ICA as an automated method for rapidly spike sorting photodiode array optical data sets removes one of the main hindrances to the widespread use of optical recording with fVSDs to study neuronal networks in invertebrate and suitable vertebrate preparations.

METHODS

Dissection

Tritonia diomedea were obtained from Living Elements (Vancouver, British Columbia, Canada) and *Aplysia californica* were obtained from the National Resource for *Aplysia* facility (Miami, FL). Animals were maintained in chilled (11°C for *Tritonia*, 15°C for *Aplysia*), recirculating artificial seawater (Instant Ocean, Aquarium Systems, Mentor, OH) systems prior to experiments. For *Tritonia*, the fused cerebral–pleural ganglia and the pedal ganglia and, for *Aplysia*, the cerebral, pleural, pedal, and buccal ganglia were removed from the animal and excess connective tissue was removed. The ganglia were then pinned to the coverslip floor of a recording chamber (WPI, Sarasota, FL) that was coated with a thin layer of Sylgard. For both preparations, the connective tissue sheath overlying the ganglion of interest was then removed using fine forceps and scissors to allow neuronal impalement with intracellular electrodes. A suction electrode was attached to a peripheral nerve to allow the stimulation of motor patterns.

Optical recording

In most experiments, ganglia were stained with 0.2 mg/ml of the voltage-sensitive absorption dye RH-155 (Anaspec, San Jose, CA), dissolved in artificial seawater for 5 to 10 min, and then perfused with artificial seawater containing 0.02 mg/ml RH-155 throughout the experiment (Parsons et al. 1991). In other experiments we stained with artificial seawater containing 0.03 mg/ml RH 155 for 1–2 h and then continued perfusing this concentration of dye throughout the experiment. During experiments the temperature was maintained between 10.0 and 11.5°C for *Tritonia* and between 14.0 and 16.0°C for *Aplysia* by passing the perfusion solution through a feedback-controlled, in-line Peltier cooling system (Model SC-20; Warner Instruments, Hamden, CT) using a peristaltic pump (Model 720; Instech Laboratories, Plymouth Meeting, PA). Recording chamber saline temperature was monitored with a Bat-12 thermometer fitted with an IT-18 microprobe (Physitemp Instruments, Clifton, NJ).

An Olympus tungsten– halogen 100-W lamp house (Olympus, Tokyo) powered by an Olympus TH4 DC power supply was used for illuminating the preparation. Light from the lamp house was passed through the adjustable base diaphragm of an Olympus BX51WI upright microscope, filtered by a 725/50 band-pass filter (Chroma Technology, Rockingham, VT), and then passed through an electronic shutter (Model VS35; Vincent Associates, Rochester, NY), and a 0.9 numerical aperture (NA) Abbe achromat substage condenser (Nikon, Tokyo) before reaching the preparation. Light from the preparation was collected by a ×20 0.95 NA water-immersion objective lens (Olympus) and was then

directed through a phototube to reach either the photodiode array or a parfocal Microfire digital camera (Optronics, Goleta, CA).

Optical recording experiments were performed with a PDA-III photodiode array (RedShirtImaging, Decatur, GA). The PDA-III contains 464 photodiodes and the full set was sampled at 1.6 kHz. The output of the photodiodes was AC coupled with a 2-s time constant filter in the PDA hardware and then multiplied 100-fold before being digitized with a 14-bit resolution AD board. Both optical and sharp electrode data were acquired and viewed using the RedShirtImaging Neuroplex software. Raw data traces were filtered in Neuroplex (Butterworth band-pass between 5 and 100 Hz) before being exported as text files for ICA processing. Further technical details of our optical recording procedure can be found in Frost et al. (2011).

Intracellular recording

Intracellular recordings were obtained with 15- to 30-MΩ electrodes filled with 3 M KCl or 3 M K-acetate connected to a Dagan IX2-700 dual intracellular amplifier (Dagan, Minneapolis, MN). The resulting signals were digitized at 1,600 Hz along with the optical data and saved to Neuroplex files.

Computational analysis

ICA was performed in MATLAB (The Math Works, Natick, MA) on optical recording data exported as text files from Neuroplex. Most of the ICA processing was done using a 3.2-GHz HP Z400 64-bit PC workstation with 8 GB RAM running Windows XP Professional ×64. On this machine, ICA can process a 60-s file of 464 optical traces digitized at 1,600 Hz into a set of 464 independent components in about 10 min.

We use Infomax ICA (Bell and Sejnowski 1995) with the natural gradient feature of Amari, Cichocki, and Yang, implemented in Delorme and Makeig (2004), freely available at http://cnl.salk.edu/Research/ICA/Optical/. Infomax ICA is an iterative algorithm that yields a “weight matrix,” representing a linear transformation of the optical data into components that are maximally statistically independent from each other. The independent components are produced by multiplying the resulting weight matrix by the matrix of the filtered optical data. The values of the rows of the weight matrix represent the contributions made by the 464 diodes to each independent component.

The component traces returned by ICA fall into three categories: *1*) those that appear to represent separated neuronal activity (they contain action potentials), *2*) those that contain optical artifacts, and *3*) those that contain background noise. To simplify inspection of the ICA results, a MATLAB program was written that automatically identifies, ranks, and displays the components likely to contain action potentials, based on the asymmetry of their distribution around the baseline. The user can also separately view the remaining components returned by ICA. The spatial location of each component on the diode array, and therefore the position of the recorded neuron in the ganglion, is recovered from the corresponding column of the inverse weight matrix (Brown et al. 2001).

To illustrate ICA’s ability to accurately find the independent components in mixed, redundant, and noisy data, we linearly mixed three signals: two intracellular recordings of spiking activity in *Tritonia* pedal ganglion neurons and one trace of white noise (Fig. 1). The weights used to make each of the three signal mixtures are shown above each of the mixed traces. When ICA was applied to this data set, it returned three independent components that exactly corresponded to the original signals. The optical imaging data that we acquired with a photodiode array is essentially similar to the mixed traces shown in Fig. 1, but with 464 mixed, redundant, and noisy traces instead of only three.

To assess the accuracy of ICA, we used a custom MATLAB program that finds the independent component returned by ICA that best matches, spike-for-spike, the intracellularly recorded trace. The two traces are then displayed, with any potential mismatches (optical spikes in the component that are not present in the intracellular data or vice versa) highlighted for visual inspection.

RESULTS

ICA performs spike sorting and returns spatial maps of the independent component

In photodiode array optical recording experiments with invertebrate ganglia, large neurons can be redundantly recorded by many photodiodes and individual photodiodes may record action potentials from multiple neurons (Fig. 2*A*). We use ICA to transform these mixed and redundant raw optical recordings into a new set of traces (components), with many traces containing the action potentials of individual neurons. ICA returns the same number of components as input channels, in our case, 464. Typically, several dozen to >100 of these components contain action potentials from what appear to be single neurons (Fig. 2*B*), with the remainder of the components containing either artifacts (also sorted by ICA into separate traces) or noise.

To determine the location of an ICA component on the photodiode array, we used the spatial map generated from a column of the inverse weight matrix showing the contribution of that component to the mixed optical signals recorded by each diode (Fig. 2*C*). For the components containing action potentials, the diode maps typically outlined a circular region of a few diodes (Fig. 2*C*), which often corresponded to a visible neuron in a photograph of the ganglion superimposed over the diode positions in Neuroplex (Fig. 2*D*). The neuron-shaped maps were not imposed by ICA, which had no knowledge of the underlying topology of the array.

Validating the accuracy of ICA spike sorting

The usefulness of ICA for spike sorting optical recording data (Fig. 2) depends on its accuracy—how well the component traces correspond to the actual spiking activity of individual neurons. To evaluate this, we obtained simultaneous intracellular and optical recordings from neurons in the central ganglia of two different species of marine mollusk, *Tritonia diomedea* and *Aplysia californica*.

In the first experimental protocol, we imaged from the dorsal surface of a *Tritonia* pedal ganglion while evoking action potentials in one or two impaled pedal ganglion neurons using current injected through the microelectrodes (Fig. 3*A*). Figure 3*Bi* shows the pre-ICA optical recordings from 12 diodes that covered the ganglion region occupied by two impaled neurons. Each neuron was recorded by several diodes (redundant signals) and, because the two neurons were adjacent to one another, some diodes recorded the action potential activity of both neurons (mixed signals, Fig. 3*Bi*, diodes 355 and 367). In this experiment, the electrodes were used to pass current to make the neurons fire separately, and at times simultaneously, to force mixed signals (Fig. 3*Bii*). ICA was performed on the full 464-channel optical data set. Two of the independent components returned by ICA corresponded spike-for-spike with the action potentials recorded in the two impaled neurons (Fig. 3, *Bii* and *Biii*). In all cases of intracellular current injection in *Tritonia* (11 neurons in seven preparations), ICA returned a component that exactly matched the firing, spike-for-spike, of one of the intracellularly impaled neurons.

Next, we tested the accuracy of ICA performed on pedal ganglion optical recordings of *Tritonia* swim motor programs evoked by stimulation of a peripheral nerve (pedal nerve 3, 10 V, 10 Hz, 2 s, 5 ms pulses). Such recordings contain a much higher level of action

potential activity than that of the prior quiescent preparations, where only one or two neurons were excited by direct intracellular stimulation. In the same preparation as shown in the prior figure, the spiking activity of each of two adjacent impaled neurons was detected by many diodes (Fig. 4*Ai*) and at least three diodes (354, 355, and 367) detected the spiking activity of both neurons. The simultaneous intracellular recordings from the two neurons during the swim motor program showed that one neuron fired many bursts of action potentials (Fig. 4*Aii*, *top trace*), whereas the other neuron was inhibited during the motor program (Fig. 4*Aii*, *bottom trace*). Two of the neuronal independent components returned by ICA (Fig. 4*Aiii*) corresponded exactly, spike-for spike, to the intracellularly recorded activity of the two impaled neurons (expanded view shown in Fig. 4, *Bi* and *Bii*). Note that in the expanded view shown in Fig. 4, *Bi* and *Bii* the spike undershoots are clearly present in the components, showing that ICA preserves such features of the membrane potential information present in the filtered optical data. In all seven *Tritonia* preparations in which intracellular recording and imaging were performed simultaneously during nerve-evoked swim motor programs, ICA returned independent components that exactly matched, spike-for-spike, the firing in the impaled neurons (nine of nine neurons).

Next, to evaluate the spike sorting accuracy of ICA in another species, we repeated these testing paradigms in a second widely used invertebrate model preparation, the marine mollusk *Aplysia californica*. Again there was perfect correspondence between the intracellularly recorded action potentials and the spikes of the matching independent component in experiments where we drove impaled neurons while simultaneously obtaining optical recordings from the pedal or buccal ganglia of *Aplysia californica* (Fig. 5*A*; nine neurons in six preparations). Similar results were obtained when recording intracellularly from neurons of the pedal and buccal ganglia of *Aplysia* while imaging optically during firing activity evoked by peripheral nerve stimulation (pedal nerve 9 or buccal nerve 5, respectively) or during ongoing motor programs. In all five such preparations, the optical spikes of one of the independent components corresponded exactly, spike-for-spike, to the intracellularly recorded activity of the impaled neuron during the motor program (Fig. 5*B*). Note that the optical artifact present in the optical data in Fig. 5B is not present in the matching component returned by ICA. This feature of ICA will be demonstrated further in Fig. 7.

In a further validation test, in one experiment we performed ICA on concatenated optical data files from five separate data acquisitions obtained over a period of 24 min while simultaneously recording from two *Tritonia* pedal ganglion neurons with intracellular electrodes. Of the neuronal independent components returned by ICA, two corresponded exactly, spike-for-spike, across all recordings with the action potentials in the two impaled neurons (Fig. 6). This result demonstrates that ICA can be used to accurately track the firing of large numbers of individual neurons over several data files acquired separately in the same preparation, such as might be desirable in studies of the effects of synaptic plasticity or drugs on network activity over time.

In experiments where we simultaneously recorded intracellularly and optically, the spatial maps for the corresponding independent components always matched the location of the impaled neurons on the photograph of the ganglion superimposed in Neuroplex (Fig. 2, *C* and *D*). This correspondence of the spatial maps of the matching components to the array positions of the impaled neurons represents further validation of the accuracy of ICA.

ICA also sorts optical artifacts into independent components

Finally, the imaging data recorded with a photodiode array often contain optical artifacts stemming from vibration or other sources that can be many times larger than the optical signals produced by action potentials. A useful feature of ICA is that such recorded artifacts

are themselves isolated into separate independent components, resulting in artifact-free neuronal independent component traces (Fig. 7).

Methods for optimizing the number of returned neuronal independent component

The number of neurons recovered by ICA from the raw data are limited by the number of detectors, the signal-to-noise ratio, and the independence of the data. Prefiltering the raw optical data to remove both high- and low-frequency noise (Butterworth band-pass between 5 and 100 Hz) consistently increased the number of neuronal independent components returned by ICA (data not shown), partly by increasing the signal-to-noise ratio of the data. Removing low-frequency noise (e.g., large-amplitude, slowly changing signals) from the optical data by high-pass filtering may also improve ICA's performance by increasing the independence of the components (Hyvarinen et al. 2001). Optimal filter settings may vary depending on the preparation and thus should be determined empirically. In addition, when ICA was run on longer data files (e.g., 60 to 90 s) it returned more neuronal independent components than it did when run on the same data files truncated to shorter lengths (e.g., 10 to 30 s; data not shown). Finally, we found that including more of the spontaneous spiking activity that occurs before an applied nerve stimulus also often increased the number of neuronal independent components returned by ICA (data not shown). This may be a result of greater independence between neurons when they are firing spontaneously than when many are bursting in near synchrony during a motor program. In summary, we found that prefiltering the optical data, increasing the amount of data collected, and including prestimulus spontaneous activity all could increase the number of neuronal independent components returned by ICA.

DISCUSSION

ICA has been applied to data sets generated by several techniques for monitoring neural activity, including: electroencephalography (Delorme et al. 2007), calcium imaging of many individual neurons (Mukamel et al. 2009; Schultz et al. 2009), calcium and voltage imaging of many individual neurons (Reidl et al. 2007), functional magnetic resonance imaging (Duann et al. 2002), cortical and blood vessel intrinsic signal imaging (Siegel et al. 2007), and invertebrate neuronal action potential imaging with a photodiode array and an fVSD (Brown et al. 2001, 2008). To our knowledge, the present study represents the first time that the accuracy of the independent components returned by ICA has been validated using simultaneous optical and intracellular recordings [previously reported in an abstract (Frost et al. 2008)]. For 34 of 34 neurons in *Tritonia* and *Aplysia* impaled with an intracellular electrode during optical recording, one of the independent components returned by ICA corresponded exactly, spike-for-spike, to the action potentials recorded from the impaled neuron. This result validates the use of ICA for rapid, automated spike sorting of optical imaging data sets and thus establishes fVSD imaging combined with ICA as a powerful technique for large-scale studies of suitable neuronal networks.

Although ICA is a powerful method for spike sorting optical recording data, it does have certain limitations. For example, when neurons are aligned vertically such that the exact same diodes record the neurons' optical signals in the same ratio on all the diodes, it cannot separate them into different independent components (Brown et al. 2001). In such cases, the spikes from each neuron appear together in one neuronal independent component (where they can often be visually distinguished on the basis of spike height). Further, in cases where multiple spatially separate neurons fire exactly synchronous, identically shaped action potentials, such as in response to a stimulus train applied to a nerve in which they have their axons (antidromic stimulation), ICA may sort these synchronous action potentials into a single independent component (Brown et al. 2001). Next, ICA performs poorly, in terms of the numbers of neuronal components returned, on small data sets because insufficient

information from each neuron is present in the data for ICA to separate them from one another and from other source signals. Thus acquiring longer data files, up to a point (e.g., 60 to 90 s), will lead to more resolved neuronal components. Although the number of neuronal independent components returned by ICA increased with increasing data length, the spike sorting was consistently accurate. For example, even files as short as 10 s returned a component that accurately matched, spike-for-spike, a simultaneously impaled neuron (data not shown). Finally, ICA cannot find more neurons than the number of detectors in the recording device. This was not an issue for the present study because we always recorded the activity of fewer than 464 neurons with our 464-element photodiode array.

ICA represents a substantial improvement over a previous spike sorting method for fVSD imaging data, which required extensive human involvement and could take several days per data file (Cohen et al. 1989; Yamada et al. 1992). It is a fast and fully automated method for determining the source signals from mixed and redundant optical recording data. Increases in computing power have shortened the time required to perform ICA on large optical recording data files from several hours to just a few minutes. Thus it is now possible to obtain and use ICA results during the course of ongoing experiments. Using the combination of fVSD imaging and ICA we can now routinely and accurately monitor the spiking activity of several dozen to >100 neurons in the central ganglia of *Tritonia* and *Aplysia*. Since each individual neuron is sorted into a separate component, instantaneous frequency plots for each neuron can be generated, which cannot be accomplished from noisy and mixed raw optical data traces. Additionally, by performing ICA on concatenated optical files (see Fig. 6), it is possible to accurately track the activity of many individual neurons over multiple bouts of optical recording separated over time.

For many decades, intracellular electrode recording has limited the view of invertebrate networks to the small number of neurons that can be impaled at one time. The large-scale imaging studies of Cohen and colleagues (London et al. 1986, 1987; Salzberg et al. 1977; Wu et al. 1988, 1994a,b; Zecevic et al. 1989) and, more recently, Kristan and colleagues (Brigg-man and Kristan Jr 2006; Briggman et al. 2005; Taylor et al. 2003) have elegantly demonstrated the power and appeal of large-scale optical recording with voltage-sensitive dyes. Yet, despite these studies, voltage-sensitive dye optical imaging has not been widely adopted. The application of ICA for spike sorting fVSD optical recordings (Brown et al. 2001, 2008; Frost et al. 2011), demonstrated further and validated for the first time in the present study, establishes a major new tool for those seeking to explore a host of network-level issues that are difficult to approach with traditional neurophysiological techniques. For example, do the numbers of neurons participating in a network change within or between instances of network operation? How many neurons are excited or inhibited by a given neuron and how does this change with synaptic plasticity or pharmacological manipulation? What are the network consequences of learning and memory? How multifunctional are the neurons of a given network? The present validation of the accuracy of Infomax ICA for rapid spike sorting of individual neurons from fVSD optical recording data establishes a powerful tool for addressing such important network-level questions.

Acknowledgments

We thank Dr. Jean Wang for technical assistance and Drs. Eran Mukamel, J. R. Duann, Tony Bell, and Lise Eliot for helpful discussions.

GRANTS

This research was supported by National Institute of Neurological Disorders and Stroke Grant NS-060921 to W. N. Frost, Dart Foundation Fellowships at the Marine Biological Laboratory to W. N. Frost, and a Howard Hughes Medical Institute grant to T. J. Sejnowski.

References

Bell AJ, Sejnowski TJ. An information-maximization approach to blind separation and blind deconvolution. Neural Comput 1995;7:1129–1159. [PubMed: 7584893]

Briggman KL, Abarbanel HD, Kristan WB Jr. Optical imaging of neuronal populations during decision-making. Science 2005;307:896–901. [PubMed: 15705844]

Briggman KL, Kristan WB Jr. Imaging dedicated and multifunctional neural circuits generating distinct behaviors. J Neurosci 2006;26:10925–10933. [PubMed: 17050731]

Brown, GD.; Yamada, S.; Nakashima, M.; Moore-Kochlacs, C.; Sejnowski, TJ.; Shiono, S. UCSD Technical Report INC-08-001. La Jolla, CA: Institute for Neural Computation, Univ. of California San Diego; 2008 Oct. Independent component analysis of optical recordings from *Tritonia* swimming neurons.

Brown GD, Yamada S, Sejnowski TJ. Independent component analysis at the neural cocktail party. Trends Neurosci 2001;24:54–63. [PubMed: 11163888]

Cleary LJ, Byrne JH, Frost WN. Role of interneurons in defensive withdrawal reflexes in Aplysia. Learn Mem 1995;2:133–151. [PubMed: 10467571]

Cohen L, Hopp HP, Wu JY, Xiao C, London J. Optical measurement of action potential activity in invertebrate ganglia. Annu Rev Physiol 1989;51:527–541. [PubMed: 2653195]

Cohen LB, Salzberg BM. Optical measurement of membrane potential. Rev Physiol Biochem Pharmacol 1978;83:35–88. [PubMed: 360357]

Cropper EC, Evans CG, Hurwitz I, Jing J, Proekt A, Romero A, Rosen SC. Feeding neural networks in the mollusc *Aplysia*. Neuro-Signals 2004;13:70–86. [PubMed: 15004426]

Delorme A, Makeig S. EEGLAB: an open source toolbox for analysis of single-trial EEG dynamics including independent component analysis. J Neurosci Methods 2004;134:9–21. [PubMed: 15102499]

Delorme A, Sejnowski T, Makeig S. Enhanced detection of artifacts in EEG data using higher-order statistics and independent component analysis. NeuroImage 2007;34:1443–1449. [PubMed: 17188898]

Duann JR, Jung TP, Kuo WJ, Yeh TC, Makeig S, Hsieh JC, Sejnowski TJ. Single-trial variability in event-related BOLD signals. NeuroImage 2002;15:823–835. [PubMed: 11906223]

Falk CX, Wu JY, Cohen LB, Tang AC. Nonuniform expression of habituation in the activity of distinct classes of neurons in the *Aplysia* abdominal ganglion. J Neurosci 1993;13:4072–4081. [PubMed: 8366360]

Frost WN, Moore-Kochlacs C, Hill ES, Wang J, Sejnowski TJ. Simultaneous intracellular and optical recordings confirm blind separation of single neurons by independent component analysis. Soc Neurosci Abstr 2008;371:16.

Frost, WN.; Wang, J.; Brandon, CJ.; Moore-Kochlacs, C.; Sejnowski, TJ.; Hill, ES. Use of fast-responding voltage-sensitive dyes for large-scale recording of neuronal spiking activity with single-cell resolution. chapt. 5. In: Canepari, M.; Zecevic, D., editors. Membrane Potential Imaging in the Nervous System: Methods and Applications. 1st ed.. New York: Springer; 2011. p. 53-60.

Getting PA. Neural control of swimming in Tritonia. Symp Soc Exp Biol 1983;37:89–128. [PubMed: 6679124]

Hickie C, Cohen LB, Balaban PM. The synapse between LE sensory neurons and gill motoneurons makes only a small contribution to the Aplysia gill-withdrawal reflex. Eur J Neurosci 1997;9:627–636. [PubMed: 9153569]

Hyvarinen, A.; Karhunen, J.; Oja, E. Independent Component Analysis. New York: Wiley-Interscience; 2001. p. 481

Jung TP, Makeig S, McKeown MJ, Bell AJ, Lee TW, Sejnowski TJ. Imaging brain dynamics using independent component analysis. Proc IEEE 2001;89:1107–1122.

Kojima S, Hosono T, Fujito Y, Ito E. Optical detection of neuromodulatory effects of conditioned taste aversion in the pond snail *Lymnaea stagnalis*. J Neurobiol 2001;9:118–128. [PubMed: 11598919]

Lewicki MS. A review of methods for spike sorting: the detection and classification of neural action potentials. Network 1998;9:R53–R78. [PubMed: 10221571]

London JA, Zecevic D, Cohen LB. Simultaneous monitoring of activity of many neurons from invertebrate ganglia using a multielement detecting system. Soc Gen Physiol 1986;40:115–131.

London JA, Zecevic D, Cohen LB. Simultaneous optical recording of activity from many neurons during feeding in Navanax. J Neurosci 1987;7:649–661. [PubMed: 2435862]

Mukamel EA, Nimmerjahn A, Schnitzer MJ. Automated analysis of cellular signals from large-scale calcium imaging data. Neuron 2009;63:747–760. [PubMed: 19778505]

Nakashima M, Yamada S, Shiono S, Maeda M, Satoh F. 448-detector optical recording system: development and application to Aplysia gill-withdrawal reflex. IEEE Trans Biomed Eng 1992;39:26–36. [PubMed: 1572678]

Neunlist M, Peters S, Schemann M. Multisite optical recording of excitability in the enteric nervous system. Neurogastroenterol Motil 1999;11:393–402. [PubMed: 10520170]

Nikitin ES, Balaban PM. Optical recording of odor-evoked responses in the olfactory brain of the naive and aversively trained terrestrial snails. Learn Mem 2000;7:422–432. [PubMed: 11112801]

Obaid AL, Koyano T, Lindstrom J, Sakai T, Salzberg BM. Spatiotemporal patterns of activity in an intact mammalian network with single-cell resolution: optical studies of nicotinic activity in an enteric plexus. J Neurosci 1999;19:3073–3093. [PubMed: 10191324]

Obaid AL, Nelson ME, Lindstrom J, Salzberg BM. Optical studies of nicotinic acetylcholine receptor subtypes in the guinea-pig enteric nervous system. J Exp Biol 2005;208:2981–3001. [PubMed: 16043603]

Parsons TD, Salzberg BM, Obaid AL, Raccuia-Behling F, Kleinfeld D. Long-term optical recording of patterns of electrical activity in ensembles of cultured *Aplysia* neurons. J Neurophysiol 1991;66:316–333. [PubMed: 1919674]

Popescu IR, Frost WN. Highly dissimilar behaviors mediated by a multifunctional network in the marine mollusk *Tritonia diomedea*. J Neurosci 2002;22:1985–1993. [PubMed: 11880529]

Reidl J, Starke J, Omer DB, Grinvald A, Spors H. Independent component analysis of high-resolution imaging data identifies distinct functional domains. NeuroImage 2007;34:94–108. [PubMed: 17070071]

Salzberg BM, Grinvald A, Cohen LB, Davila HV, Ross WN. Optical recording of neuronal activity in an invertebrate central nervous system: simultaneous monitoring of several neurons. J Neurophysiol 1977;40:1281–1291. [PubMed: 925730]

Schemann M, Michel K, Peters S, Bischoff SC, Neunlist M. Cutting-edge technology. III. Imaging and the gastrointestinal tract: mapping the human enteric nervous system. Am J Physiol Gastrointest Liver Physiol 2002;282:G919–G925. [PubMed: 12016115]

Schultz SR, Kitamura K, Post-Uiterweer A, Krupic J, Hausser M. Spatial pattern coding of sensory information by climbing fiber-evoked calcium signals in networks of neighboring cerebellar Purkinje cells. J Neurosci 2009;29:8005–8015. [PubMed: 19553440]

Siegel RM, Duann JR, Jung TP, Sejnowski T. Spatiotemporal dynamics of the functional architecture for gain fields in inferior parietal lobule of behaving monkey. Cereb Cortex 2007;17:378–390. [PubMed: 16603713]

Takahashi S, Anzai Y, Sakurai Y. A new approach to spike sorting for multi-neuronal activities recorded with a tetrode: how ICA can be practical. Neurosci Res 2003;46:265–272. [PubMed: 12804787]

Taylor AL, Cottrell GW, Kleinfeld D, Kristan WB Jr. Imaging reveals synaptic targets of a swim-terminating neuron in the leech CNS. J Neurosci 2003;23:11402–11410. [PubMed: 14673004]

Tsau Y, Wu JY, Hopp HP, Cohen LB, Schiminovich D, Falk CX. Distributed aspects of the response to siphon touch in Aplysia: spread of stimulus information and cross-correlation analysis. J Neurosci 1994;14:4167–4184. [PubMed: 8027769]

Vanden Berghe P, Bisschops R, Tack J. Imaging of neuronal activity in the gut. Curr Opin Pharmacol 2001;1:563–567. [PubMed: 11757810]

Wu JY, Cohen LB, Falk CX. Neuronal activity during different behaviors in Aplysia: a distributed organization? Science 1994a;263:820–823. [PubMed: 8303300]

Wu JY, London JA, Zecevic D, Hopp HP, Cohen LB, Xiao C. Optical monitoring of activity of many neurons in invertebrate ganglia during behaviors. Experientia 1988;44:369–376. [PubMed: 3286282]

Wu JY, Tsau Y, Hopp HP, Cohen LB, Tang AC, Falk CX. Consistency in nervous systems: trial-to-trial and animal-to-animal variations in the responses to repeated applications of a sensory stimulus in *Aplysia*. J Neurosci 1994b;14:1366–1384. [PubMed: 8120632]

Yamada S, Kage H, Nakashima M, Shiono S, Maeda M. Data processing for multi-channel optical recording: action potential detection by neural network. J Neurosci Methods 1992;43:23–33. [PubMed: 1528071]

Zecevic D, Wu JY, Cohen LB, London JA, Hopp HP, Falk CX. Hundreds of neurons in the *Aplysia* abdominal ganglion are active during the gill-withdrawal reflex. J Neurosci 1989;9:3681–3689. [PubMed: 2795148]

Zochowski M, Cohen LB, Fuhrmann G, Kleinfeld D. Distributed and partially separate pools of neurons are correlated with two different components of the gill-withdrawal reflex in *Aplysia*. J Neurosci 2000;20:8485–8492. [PubMed: 11069956]

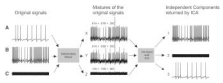

FIG. 1.

Deliberate mixing of signals illustrates the ability of independent component analysis (ICA) to blindly find source signals in mixed and redundant data. Three original signals—2 intracellular recording traces from *Tritonia* pedal ganglion neurons (*A* and *B*) and one white noise trace (*C*)—were linearly mixed. The mixing coefficient applied to each of the original signals is shown above each of the mixed traces. ICA performed on this 3 detector data set returned 3 independent components that matched the original signals.

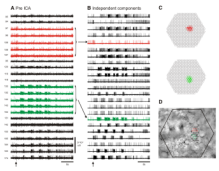

FIG. 2.

ICA extracts the spiking activity of individual neurons from mixed and redundant photodiode array optical recording data. *A*: pre-ICA; 23 traces of a 464 trace photodiode array recording of a 4 cycle swim motor program in the dorsal pedal ganglion of *Tritonia*, elicited by a stimulus to pedal nerve 3 (10 V, 5 ms pulses, 10 Hz, 1 s; arrow). Typical of such recordings, neurons large enough to be detected by many diodes are recorded redundantly (e.g., red and green traces), whereas many diodes detect signals from more than one neuron, resulting in signal mixtures. Traces were filtered in Neuroplex with a Butterworth band-pass filter (between 5 and 100 Hz). Diode numbers are shown to the *left* of the diode traces here and in subsequent figures. *B*: post-ICA; 23 of the 88 neuronal independent components returned by ICA containing recognizable neural activity are shown. The independent components shown in red and green illustrate how redundancy in the optical recordings is eliminated by ICA (see arrows). *C*: displaying the contribution of each diode to any given component (obtained from the inverse of the ICA weight matrix) indicates the location of the component, and therefore the corresponding neuron, on the photodiode array. The diode maps for the red and green components shown in *B* are displayed. *D*: the array locations of all 23 traces shown in *A* are superimposed at their recording site on the pedal ganglion.

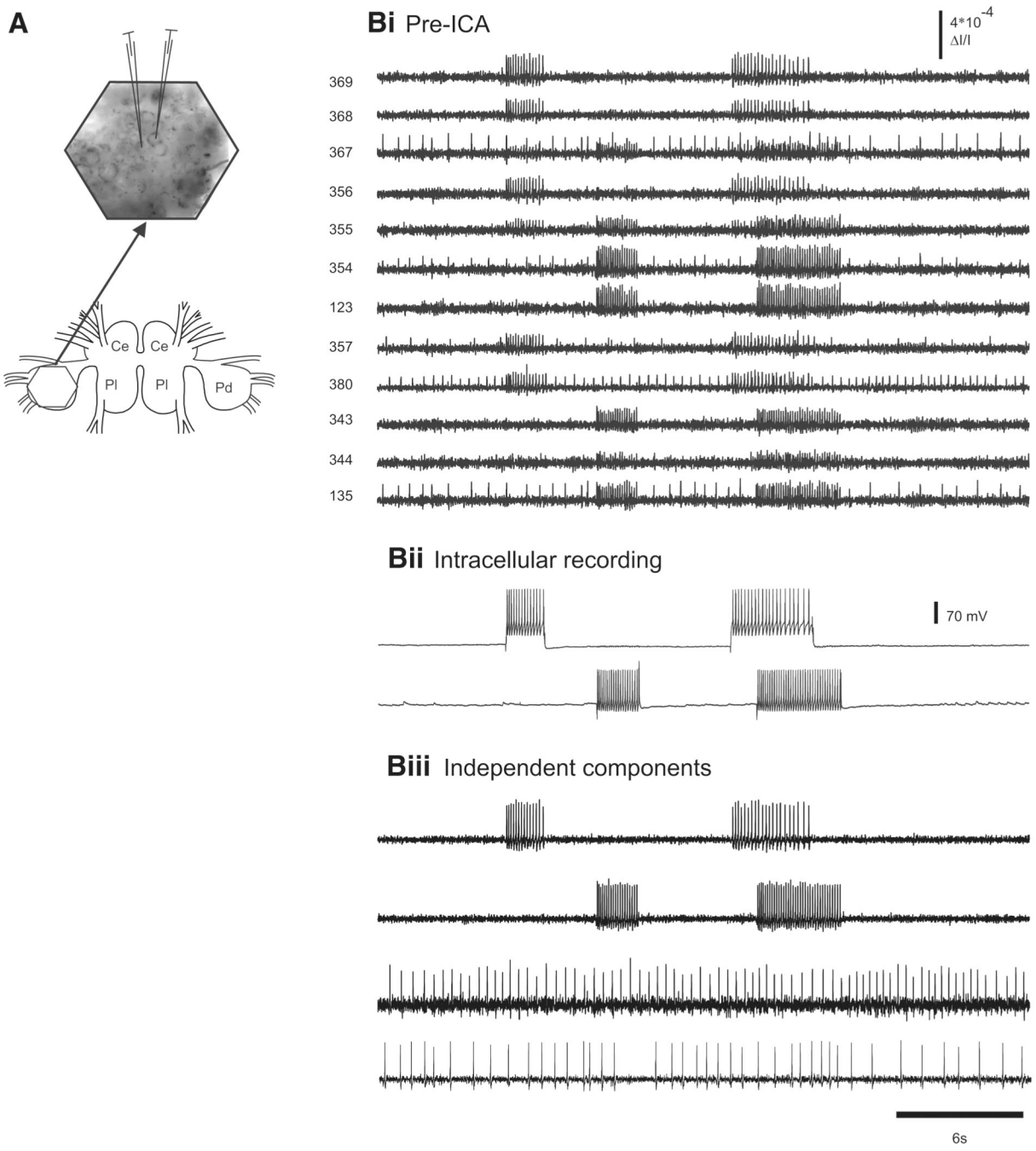

FIG. 3.

Accuracy of ICA spike sorting in a quiescent *Tritonia* preparation. *A*: illustration of the central ganglia of *Tritonia* (Ce, cerebral; Pl, pleural; Pd, pedal) and the optical recording setup. The hexagon over the left dorsal pedal ganglion (*bottom*) shows the imaged region. A larger view of the imaging area (arrow) with the image of the pedal ganglion superimposed shows the location of 2 neurons that were impaled with electrodes. *B*: accuracy of ICA spike sorting. *Bi*: pre-ICA. Current was injected into the 2 pedal ganglion neurons, making them fire trains of action potentials, which were detected optically by several diodes. Diodes 355 and 367 (adjacent diodes) each detected action potentials from both of the impaled neurons. *Bii*: intracellular recording traces from the 2 impaled neurons. *Biii*: ICA returned neuronal

independent components that represented the spiking activity of individual neurons. Among them were 2 that corresponded exactly to the intracellularly recorded action potentials in the 2 impaled neurons (*top 2 traces*). In addition, 2 other neuronal components are shown that corresponded to the spiking activity of other neurons observed in the optical data shown in *Bi*. The third component corresponds to the action potentials of one of the neurons recorded by diode 380 and the fourth component corresponds to action potentials recorded by diodes 367 and 135 (adjacent diodes).

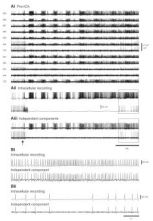

FIG. 4.

Accuracy of ICA spike sorting of a *Tritonia* swim motor program. *Ai*: pre-ICA. The spiking activity of 12 photodiodes during a swim motor program imaged in the dorsal pedal ganglion elicited by a stimulus to pedal nerve 3 (10 V, 5 ms pulses, 10 Hz, 1 s; arrow). *Aii*: intracellular recordings from 2 adjacent neurons during the swim motor program. *Aiii*: 2 of the neuronal independent components returned by ICA corresponded exactly to the 2 intracellular traces. *Bi*: expanded view of the top intracellular recording trace and its corresponding independent component (see boxes in *Aii* and *Aiii*). *Bii*: expanded view of the bottom intracellular recording trace and its corresponding independent component (see boxes in *Aii* and *Aiii*).

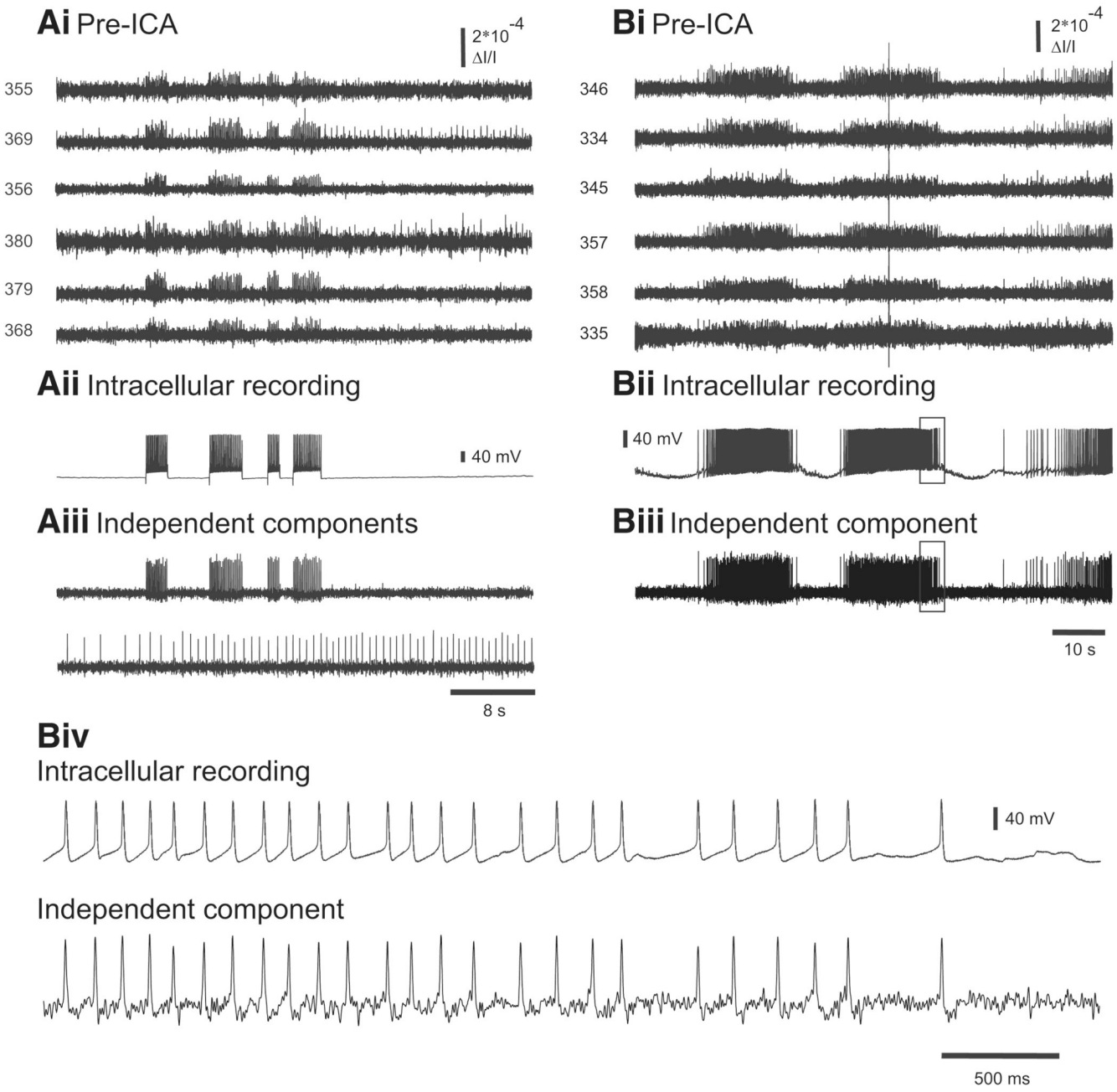

FIG. 5.

Accuracy of ICA spike sorting in *Aplysia*. *A*: validation of ICA by intracellular current injection and imaging in a quiescent preparation. *Ai*: pre-ICA. The action potentials from a neuron in the buccal ganglion driven with current injected from an intracellular electrode appear on many diodes, including 2 (369 and 380) that also detected the action potentials of another neuron. *Aii*: intracellular recording of the impaled neuron, showing 4 firing trains produced by the current injection. *Aiii*: one of the neuronal independent components (*top trace*) returned by ICA corresponded exactly to the intracellularly recorded activity of the impaled neuron. Another of the components returned by ICA (*bottom trace*) represents the activity of the other neuron whose action potentials were also detected by diodes 369 and 380 (shown in *Ai*). *B*: validation of ICA by intracellular recording and imaging during an

ongoing locomotion motor program in the *Aplysia* pedal ganglion. *Bi*: pre-ICA. The action potentials from an impaled pedal ganglion neuron during the motor program are present on many diodes. A large optical artifact is also present in the diode traces. *Bii*: intracellular recording of the impaled neuron. *Biii*: one of the neuronal independent components returned by ICA corresponded exactly with the intracellularly recorded activity of the impaled neuron. Note that the optical artifact is not present in the component. *Biv*: expanded view of the boxes in *Bii* and *Biii* showing the correspondence between the intracellularly recorded action potentials and the optical spikes of the matching independent component.

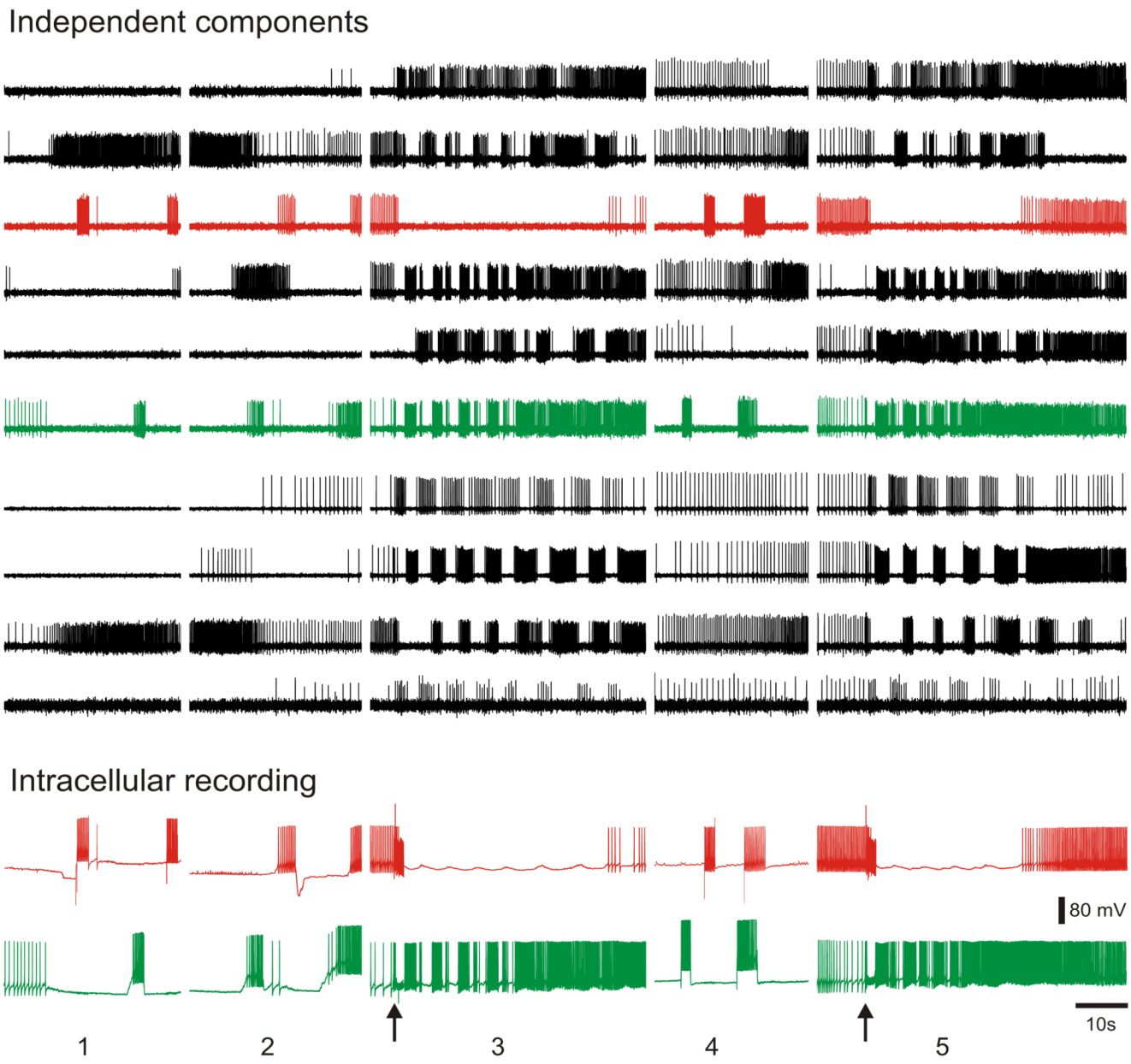

FIG. 6.

By concatenating multiple optical files, it is possible to track the activity of individual neurons over multiple imaging sessions. The *top traces* show 10 of the 45 neuronal independent components returned by ICA performed on a file concatenated from 5 separate optical files acquired from the dorsal pedal ganglion of *Tritonia* over 24 min. The different optical recording files are shown separated by spaces. The *bottom traces* show intracellular recordings from 2 impaled pedal ganglion neurons that were acquired simultaneously with the optical data. The red intracellular recording trace corresponds exactly, spike-for-spike, to the red component and the green intracellular recording trace corresponds exactly, spike for-spike, to the green component. In optical files 1, 2, and 4, current was injected into the impaled neurons to make them fire action potentials and in optical files 3 and 5, a swim motor program was elicited by pedal nerve 3 stimulation (10 V, 10 Hz, 2 s, 5 ms pulses, stimuli indicated by arrows).

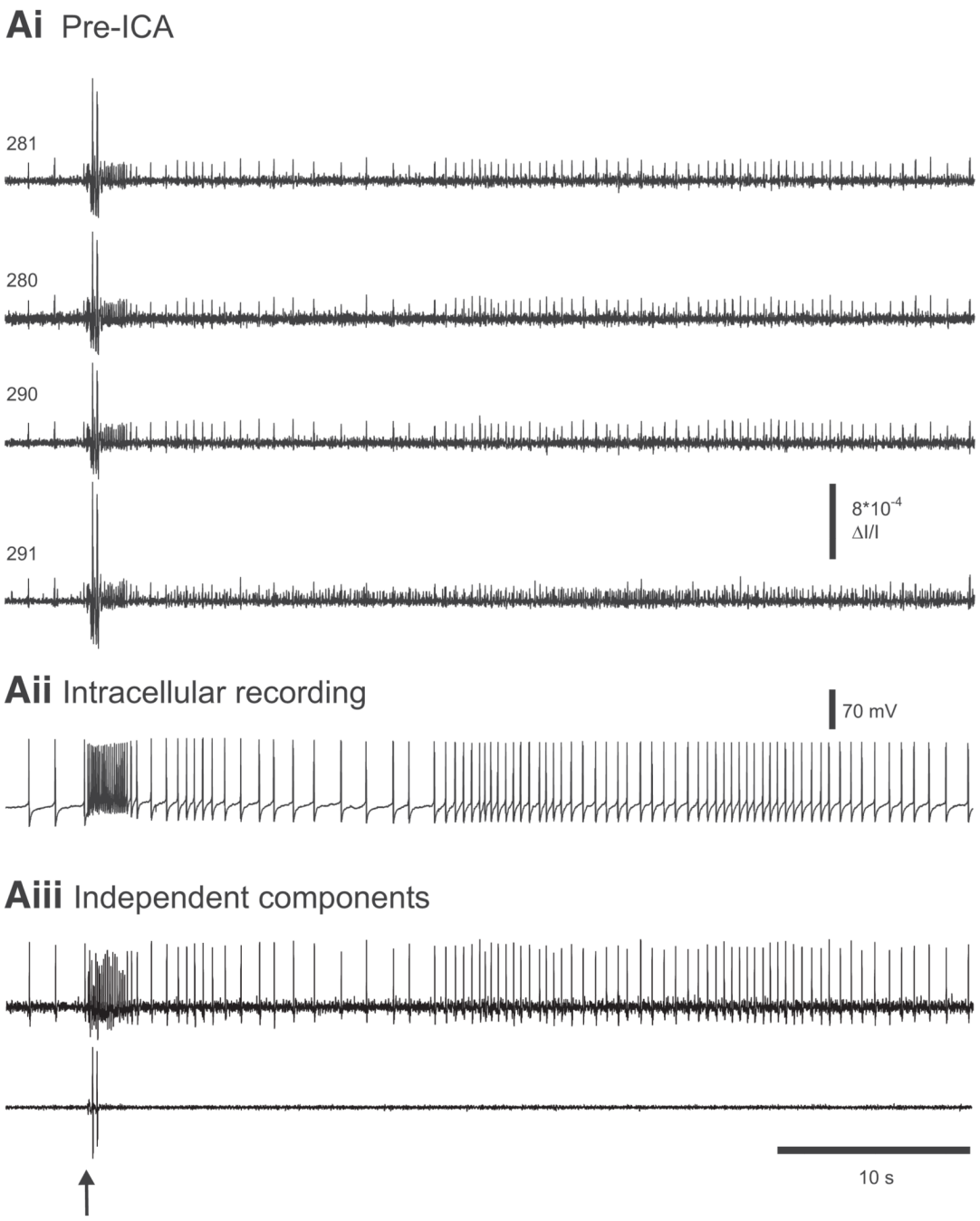

FIG. 7.

ICA removes optical artifacts. *Ai*: pre-ICA. In an experiment imaging a nerve-evoked rhythm in the pedal ganglion of *Aplysia*, several diodes contain action potentials as well as large optical artifacts. Diode numbers are shown on the *left*. *Aii*: intracellular recording of a pedal ganglion neuron. *Aiii*: among the neuronal independent components returned by ICA is one containing the activity of a single neuron that generated most of the spikes in the optical data shown in *Ai* and that corresponds exactly to the intracellular recording shown in *Aii*. Another component returned by ICA contains the artifacts present in the optical data shown in *Ai*. The arrow indicates the stimulus given to pedal nerve 9 (10 V, 5 ms pulses, 10 Hz, 2 s).